Journal of Geoscience and Environment Protection, 2023, 11, 85-113
https://www.scirp.org/journal/gep
ISSN Online: 2327-4344
ISSN Print: 2327-4336

Impact and Health Risk Assessment of Groundwater in the Vicinity of Dumpsites in Keffi Metropolis, Nigeria

Kyari Umar Donuma[1], Limin Ma[1,2*], Chengcheng Bu[1], Lartey-Young George[1]

[1]College of Environmental Science and Engineering, Tongji University, Shanghai, China
[2]Key Laboratory of Yangtze River Water Environment, Ministry of Education, Tongji University, Shanghai, China
Email: *lmma@tongji.edu.cn

How to cite this paper: Donuma, K. U., Ma, L. M., Bu, C. C., & George, L.-Y. (2023). Impact and Health Risk Assessment of Groundwater in the Vicinity of Dumpsites in Keffi Metropolis, Nigeria. *Journal of Geoscience and Environment Protection, 11,* 85-113.
https://doi.org/10.4236/gep.2023.118006

Received: July 21, 2023
Accepted: August 22, 2023
Published: August 25, 2023

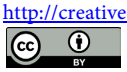

Abstract

This study investigated the hydrogeochemical characteristics of groundwater impacted by waste dumps through computation of different hydrogeological/chemical indices and related health risk assessment of major heavy metals (HVM) in relation to different population groups in Keffi Metropolis. Samples from ten (10) groundwater sources were collected for analysis. Results revealed that the concentration of major cations from the samples was in the order: $Ca^{2+} > Na^{+} + K^{+} > Mg^{2+}$, while major anionic constituents were in the order: $HCO_3^- > CO_3^{2-} > SO_4^{2-} > Cl^- > F^-$ respectively. Water quality index (WQI) computed indicated that the groundwater of the study area is not suitable for domestic purposes particularly drinking as some of the parameters exceed the WHO guidelines. Generally, the HVM hazard quotients (HQ) of non-carcinogenic (NC) and carcinogenic toxicity (TC) for both population groups were lower (HQ < 1) indicating that the groundwater within the study areas did not pose current significant risk. Non-carcinogenic risk uncertainty analysis by Monte Carlo simulations (MCS) further indicated that risk levels of HVM in GW were lower (HQ < 1). Despite the findings in this study, it is important that regular monitoring of GW quality is done in order to ensure that water is potable and prevent human health risks.

Keywords

Heavy Metals, Water Quality Index, Hydrogeochemical Facies, Municipal Waste, Irrigation

1. Introduction

Given the shortcomings of municipal water delivery systems in developing

countries, groundwater has become a reliable option for obtaining safe drinking water (Akinbile & Yusoff, 2011). In sub-Saharan Africa (SSA), dependence on groundwater resources is rapidly increasing among city dwellers due to rampant contamination of surface waterbodies (Masindi & Foteinis, 2021). Meanwhile, investigation on the status of groundwater quality has gained relatively little attention compared to global groundwater research (Munagala et al., 2020). Our search through the Web of Science (WoS) database using the advanced search tool and search string "Groundwater contamination AND Nigeria" retrieved a total of (N = 134) journal articles over the last 22 years (2000-2022) with most studies being undertaken in 2022. This revealed the recent attention given to the subject in Nigeria (**Figure 1**).

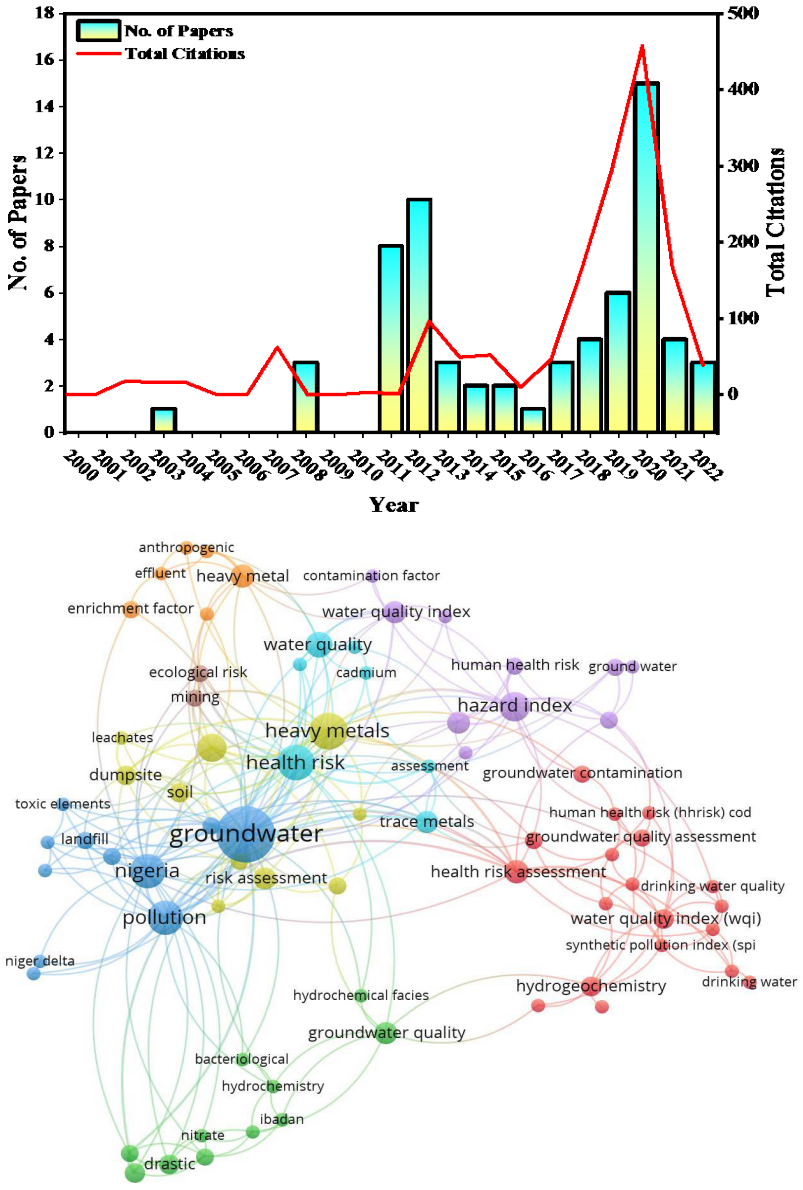

Figure 1. Publication, citation records and author keyword co-occurrence on groundwater assessment in Nigeria.

Nigeria is the most populous country in Africa with high industrial activities, which has resulted in contamination and pollution of most water resources (Pona et al., 2021). Indiscriminate disposal of municipal solid waste (MSW) in waterbodies remains a prevalent practice (Duru et al., 2019). Majority of landfills and dumpsites in Nigeria are constructed without proper engineered liners, pipes, tanks, collection equipment, or monitoring facilities which lead to leaching of leachates into groundwater (Ifeoluwa, 2019). Because leachate from the local dumpsites could be a source of pollution, areas close to such dumpsites are more likely to have contaminated groundwater (Siddiqua et al., 2022). Users of the local groundwater supply and the environment tend to be at significant danger as a result (Sanga et al., 2023). Groundwater contamination can be observed within a radius of 1000 m of an MSW site while in severe cases, this can be observed within a radius of 200 m (Aromolaran et al., 2019). Nyirenda and Mwansa (2022) observed that SO_4, NO_3, Fe, Mn and Cr concentrations in leachate samples were high near MSW sites reaching approximately 900 m from the groundwater source. Hydrogeological factors comprising rainfall, bedrock mineral weathering, the topography of dumping area and subsurface biological processes contribute towards the leaching of MSW (Kshetrimayum & Laishram, 2020). During wet seasons, the infiltration of leachate into groundwater can be very high (Mangimbulude et al., 2009).

Studies on the pollution of groundwater by leachates from MSW sites in Nigeria have been conducted to some extent. Leaching of potential toxic elements from the MSW sites often depends on the processes that fix the pollutants in soil and the seepage of contaminants into groundwater (Singh et al., 2016). (Kayode et al., 2018) evaluated the effects of MSW dumpsites on groundwater around Oke-Afa, Oshodi/Isolo areas of Lagos State, Nigeria and found high levels of heavy metals (HVMs). Aboyeji and Eigbokhan (2016), reported the effects of leachates from MSW dumpsites on the water quality of fifteen (15) boreholes and five (5) wells along the downslopes of the dumpsite around Olusosun in Lagos metropolis and found that, based on heavy metal pollution indices, the water quality was not potable compared to (WHO, 2022) guidelines. Since groundwater has become a dependable source of water supply to supplement the needs of city dwellers, the presence of traces of heavy metals (HVMs) can pose significant threats to its quality, making it unfit for use (Bolujoko et al., 2022).

Health risks associated with the consumption of contaminated water are too numerous and diverse to be glossed over, especially in developing countries where the anthropogenic impact on groundwater quality is more drastic (Sheng et al., 2022). Risk assessment processes help to determine uncertainties related to the extent and association of human health risks from exposure to HVM becomes very important. The pathways for human exposure to heavy metals in groundwater are ingestion and dermal contact (U.S. EPA., 2003) and Ghaderpoori et al. (2020) highlighted the significance of paying attention to substances that have an influence on human health through dermal pathways. Omeka and Egbueri (2023)

studied the hydrogeochemical characteristics of groundwater in Nnewi and Awka and reported that HVMs including Cd, Pb, Cu largely contributed to groundwater quality risk. In another study, Pejman et al. (2017) ranked risk factors associated to different HVMs in order of Cd > N > Pb > Ni > Cr > Zn > Cu based on their toxicities in groundwater. For the sake of human health, it is crucial to protect the quality of groundwater resources from MSW dumpsites (Mishra, et al. 2018).

Keffi metropolis of Nigeria is known to have a high dependency on groundwater resources. Thus far, an investigation into the hydrogeochemical processes of groundwater sources in the metropolis and the potential impact of MSW leachates has not been reported. Hence, this study was aimed at using various hydrogeological indices to characterize the underground water system in the area, evaluate the current and domestic agricultural potential of the water and assess the human health risks associated with the consumption of the water. The results will potentially guide further scientific investigation on groundwater sources in the study area and aid policy making on the management of solid waste and groundwater sources.

2. Materials and Methods

2.1. Study Area

2.1.1. Geology and Hydrology

According to (Yau et al., 2013), the study area is characterized by the Basement Complex, which consists of pelitic schist-amphibolites rocks and granitoids of Pan-African age. The granitoids that intrude the schists comprise granodiorite gneiss, augen granodiorite gneiss, granites and pegmatites. The grade of metamorphism in the metasedimentary rocks of the area varies from greenschists to lower amphibolite-grade facies. The orthogneisses, especially the granodiorite gneisses and augen granodiorite gneisses dominates the central and northeastern parts of the study area. The predominant geologic structural characteristics in the region consist of tectonic foliations oriented in different directions. These features, including metamorphism, folding, faults, fractures, and joints, are commonly associated with the reactivation or formation during the Pan African tectonic events. The study area is characterized by undulating terrain with the highest elevation (401 m) around the Emir's palace to the west of the metropolis. The study area is drained by Rivers Apo and Antau in addition to numerous seasonal streams within the study area.

2.1.2. Climate

Keffi metropolis experiences two major climatic conditions; a wet and a dry season. The former is experienced from April and ends in early November (covering 8 months), with its peak in July and August. Annual rainfall figures ranged from 1250 mm to 1500 mm (Olufemi et al., 2021). About 90% of the rain falls between May and September. The beginning of the dry season is marked by the southward withdrawal of the Intertropical Discontinuity (ITD) and begins in

late October and ends in March, with the months of December and January characterized by harmattan, noticeable by thin dust (Sufiyan et al., 2020). The average temperature of the area ranges from 28˚C to 29˚C in the months of July to August and 34˚C to 36˚C in the months of March and April (Sufiyan et al., 2020). The high temperature and rainfall enhance leachate formation. The relative humidity is highest (73% - 85%) in the months of July through August and lowest (52% - 60%) between January and March, which corresponds to the periods of high and low rainfalls, respectively. The rainy season (April to October) experiences Northwest trade winds, and the dry season (November to March) is characterized by the Northeast trade winds, which bring harmattan (Sufiyan et al., 2020).

2.2. Analytical Measurements

The study involved both field and laboratory activities. The field activity involved the collection of water samples from ten (10) groundwater points, (9 from hand-dug wells and 1 from a motorized borehole to serve as a control) (Figure 2), In-situ measurement of physical parameters was conducted onsite,

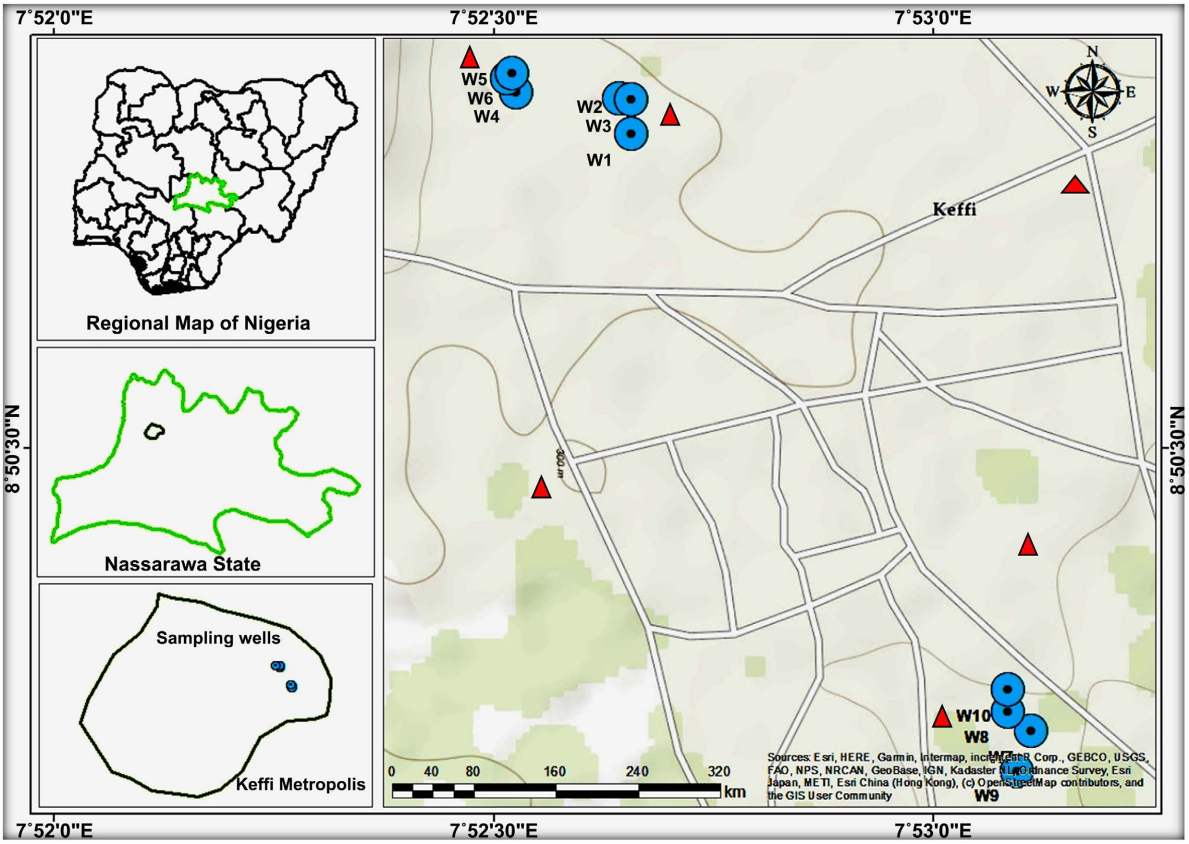

Figure 2. Present map of Keffi showing the study location as well as the dumpsites (the blue circle with black dot are the sampled Wells while the red triangles are the waste dumpsites). Ground water samples from Well 1 - 3 were obtained at Makera Fari, Samples from Well 4 - 6 were obtained at Mayanka, Samples from Well 7 - 9 were obtained at Sabon Layi Dan Jaki while the Sample 10 (control) was collected from a motorized borehole at a distance of 500 m away from the sites.

while the laboratory work involved chemical analyses of samples to determine the ion concentrations. These hand-dug wells are the primary source of domestic water supply in the study area. Water samples were collected directly from the wells into cleaned, labeled 100-ml plastic bottles that had been earlier rinsed with the particular water to be sampled. The samples were then stored in an ice-packed cooler before being taken to the laboratory. Physical parameters such as temperature, hydrogen ion (pH) concentration, electrical conductivity, and Total Dissolved Solids were determined onsite using the BLE-9909 multifunction meter. At the point of sample collection, concentrated nitric acid (HNO_3) was added to preserve the samples for metal analyses at the rate of 2 ml/L. In the laboratory, parameters including sulfate (SO_4^{2-}), alkalinity, Phosphate (PO_4^{3-}), fluoride (F^-), nitrate (NO_3^-), chloride (Cl^-) and metals including calcium (Ca), magnesium (Mg), sodium (Na), potassium (K) were analyzed following the method previously described by APHA (2012). Lead (Pb), iron (Fe), cadmium, manganese, chromium (Cr), zinc (Zn) were determined with the use of a Unicam 969 AA Atomic Absorption Spectrophotometer.

2.3. Data Analysis

Statistical summaries; mean, standard deviation, cumulative variation, kurtosis, skewness, and geometric mean were performed with Origin (OriginLab 2023, Northampton, USA) Table (S1). The Hydrogeological facies of the study area were determined using the Piper, Durov and Gibbs plots of the collected samples with the aid of Aquachem 4.0 (Waterloo Technologies, Canada). Various plots were intensively discussed, figures were presented to describe the quality of water contained in the different groundwater sources, the distribution and dominance of cations and anions in the samples and to understanding geological processes leading to the water chemistry of the study area.

2.4. Computation Using WQI and Agricultural Indices

The groundwater quality for domestic purposes was determined by computing the water quality index (WQI) and comparing the computed mean values of water quality parameters with World Health Organization (WHO) standard values. The weighted arithmetic WQI model (Tyagi et al. (2013) method was utilized to examine the impact of individual quality parameters. The water quality score, comparative weight, and the general WQI were computed using the model equations that follow:

$$Q_i = \frac{C_i}{S_i} \times 100 \tag{1}$$

$$w_i = \frac{1}{S_i} \tag{2}$$

where q_i is the quality rating of the i^{th} parameter within the given number of samples, n; C_i is the measured concentration of respective ions; S_i is the standard value of the i^{th} parameter within the given number of samples, n, and w_i represents

the relative weight of the i^{th} parameter within the given number of samples, n. The overall WQI was computed using the following:

$$\mathrm{WQI} = \frac{\sum_i^n Q_i W_i}{\sum_i^n W_i} \tag{3}$$

The WQI values computed in this study were compared with the classification according to (Akter et al., 2016) (**Table 1**). Other indices were employed to measure the suitability of the water from the study area for agricultural purposes. The indices were; total hardness (TH), percent sodium (%Na), sodium absorption ratio (SAR), permeability index (PI), and magnesium hazard (MH). The units of TH are expressed in mg/L, while %Na, SAR, RSC, PI, and MH are all expressed in m_{eq}/L Empirical equations (Equations (4)-(6)) employed in the computation of these indices are as follows:

Percent sodium, %Na, the amount of sodium expressed in percentage, that is capable of replacing Mg^{2+}, Ca^{2+} and K^{+} existing in water samples were computed using the equation after (Todd & Mays, 2004) as follows:

$$\%\mathrm{Na} = \frac{\mathrm{Na} + \mathrm{K}}{\mathrm{Ca} + \mathrm{Mg} + \mathrm{Na} + \mathrm{K}} \times 100 \tag{4}$$

Sodium absorption ratio (SAR) is employed as a means to assess alkali hazards in irrigation water, as it is linked to the absorption of Na^{+} by soil. The SAR was computed using the equation (McGeorge, 1954) as follows:

$$\mathrm{SAR} = \frac{\mathrm{Na}}{\frac{\sqrt{\mathrm{Ca} + \mathrm{Mg}}}{2}} \tag{5}$$

Magnesium hazard (MH), is the excess Mg^{2+} and Ca^{2+} that will adversely impact the soil by making it more alkaline, thus decreasing crop output (Ravikumar et al., 2010). This was calculated with the equation:

$$\mathrm{MH} = \frac{\mathrm{Mg}}{\mathrm{Ca} + \mathrm{Mg}} \times 100 \tag{6}$$

2.5. Risk Assessment

Assessing the risk of HVMs in water typically considers direct human intake and dermal contact. The adverse consequences of being exposed to heavy metals in

Table 1. Water quality index criteria.

WQI Value	Description
<50	Excellent
50 - 100	Good water
101 - 200	Poor water
201 - 300	Very poor water
>300	Water unsuitable for drinking

(Akter et al. 2016).

adults and children were calculated according to the hazard index (HI) and carcinogenic risks (CR) approach offered by the USEPA (2003) following Equations (7)-(10).

$$\text{Oral dose } (M_{\text{ing-w}}): \quad M_{\text{ing-w}} = \frac{C_s \times \text{IngR} \times \text{EF} \times \text{ED} \times \text{CF}}{\text{BW} \times \text{AT}} \tag{7}$$

$$\text{Dermal contact } (M_{\text{derm-w}}): \quad M_{\text{der-w}} = \frac{C_s \times \text{IngR} \times \text{SA} \times \text{SL} \times \text{ABS} \times \text{EF} \times \text{ED} \times \text{CF}}{\text{BW} \times \text{AT}} \tag{8}$$

$$\text{HI} = \sum \text{HQ}_i = \sum \frac{\text{ADI}_{ij}}{\text{RfD}_{ij}} \tag{9}$$

$$\text{TCR} = \sum \text{CR}_i = \sum \text{ADI}_{ij} \times \text{SF}_{ij} \tag{10}$$

where C_s is the concentration of pollutants in soil ($mg \cdot kg^{-1}$), EF is the exposure frequency (days $year^{-1}$), ED is the exposure duration (years), IngR is the receptor water ingestion rate ($mg \cdot d^{-1}$), BW is the time-averaged body weight (kg), and AT is the average time of non-carcinogenic and carcinogenic risks (days). ADI is average daily intake, SA is skin area, ABS is skin absorption factor. Specific parameters for the estimation of non-carcinogenic and carcinogenic risk are provided in (Table 2).

For non-carcinogenic risk (NCR), HI refers to all sum of HQ (Hazard Quotients) in heavy metals. HI > 1 represents the potential adverse effect on human health. For Total Carcinogenic Risk (TCR) and Carcinogenic Risk (CR), the values TCR & CR < 10^{-6}, 10^{-6} < TCR & CR < 10^{-4}, and TCR > 10^{-4} represent no health risk, no significant health risk and high health risk, respectively. The specific reference doses (RfD, $L \cdot kg^{-1} \cdot d^{-1}$) and slope factors (SF, $L \cdot kg^{-1} \cdot d^{-1}$) values are presented in (Table 3).

Risk assessment studies are mostly undertaken over a large population group, hence the potential occurrence of several uncertainties in the process. Monte Carlo simulation (MCS) is an important mathematical state-of-the-art approach for performing "what if" analyses to estimate the probabilistic risk to different

Table 2. Reference dose and cancer slope factors of heavy metals.

ID	HVM	RfD ($L \cdot d^{-1}$)		SF ($(L \cdot d^{-1})^{-1}$)		Reference
		Ingestion	Dermal contact	Ingestion	Dermal contact	
1	Fe	7.00E−03	3.00E−01	2.00E+01	-	Thongyuan et al., 2021
2	Cu	4.00E+01	1.20E+01	-	-	Tian and Wu 2019
3	Cd	1.00E−03	1.00E−05	6.10E+00	-	Tian and Wu 2019
4	Pb	1.40E−03	4.20E−01	8.50E−03	-	Tian and Wu 2019
5	Zn	3.00E+02	6.00E+01	-	-	
6	Cr	3.00E−03	1.50E−03	8.50E−03	-	Tian and Wu 2019
7	Mn	1.40E−01	6.00E−04	-	-	

HVM—Heavy metal; RfD—Reference dose; SF—Slope factor.

Table 3. Human health risk exposure parameters.

Parameters	Description	Units	Values		Reference
			Adult	Children	
IRs	Ingestion rate of water	$L \cdot d^{-1}$	2.2	1.2	(Custodio et al. 2020)
EF	Exposure frequency	$d \cdot a^{-1}$	350	320	
ED	Exposure duration	a	70	6	
BW	Average body weight	kg	70	15.9	(Custodio et al. 2020)
AT	Average exposure time	d	365 × ED (non-carcinogenic) 365 × 70 (carcinogenic)		(Meng et al. 2021)
SA	Surface area of skin	cm^2	18,000	6600	(Custodio et al. 2020)
AF	Skin adherence factor	$mg \cdot (cm^2 \cdot d)^{-1}$	0.58	1	(Custodio et al. 2020)
ABS	Dermal absorption factor	unitless	0.001 (non-carcinogenic) 0.004-(non-carcinogenic for Pb) 0.01 (carcinogenic)		(Custodio et al. 2020)

population groups (Qiu et al., 2023). It enables evaluation of the considerable variation and lack of certainty surrounding several parameters used for different procedures and has been applied in human health risk assessment for decades. For this study, MCS was applied to predict uncertainties related to the calculated non-carcinogenic risk of metalloids in adults and children. Oracle Crystal Ball® (version 11.1.2.3419.0), which is an add-in tool, was run in Microsoft Office Excel 2016 and used to estimate the MCS over 10,000 iterations, which are anticipated to estimate more stable outputs.

3. Results and Discussion

3.1. Physicochemical Factors

Statistical summary of the physicochemical factors for water samples is presented in (**Table 4**). The electric conductivity (Udiba et al.) of the groundwater samples ranged from 116 - 3850 μS/cm, with an average of 1914.40 μS/cm. The pH values were in the range of 6.31 - 7.38 with an average of 6.92, Ca^{2+} in the range of 35.8 - 135.7 with an average value of 90.94 mg/l, Mg^{2+} ranges between 3.7 - 40.92 mg/l with an average value of 18.88 mg/l, Na^{+} ranges between 9.5 - 103.9 mg/l with an average value of 58.05 mg/l, K ranges from 2.8 - 17.9 mg/l with an average value of 12.58 mg/l, Cl ranges from 1.9 - 54.9 mg/l with an average value of 13.69 mg/l, $CaCO_3$ ranges from 49.5 - 208 mg/l with an average value of 107.85 mg/l, SO_4 ranges from 5.2 - 23.26 mg/l with an average value of 13.37 mg/l, and PO_4 ranges from 2.4 - 36.6 mg/l with an average value of 3.66 mg/l. It can be observed that parameters such as EC of GW1-GW5 and GW8 exceeded the standard limits, Ca^{2+} of GW 1, GW4, GW, and GW7-GW8 exceeded the limits; and the value of K^{+} of GW5, GW8, and GW9 exceeded the standard limits of (WHO, 2022). It can be concluded that this occurred as a result

Table 4. Statistical analysis of water quality data.

Samples	Mean	Standard Deviation	Skewness	Kurtosis	Coefficient of Variation
Ec (µS/cm)	1914.40	990.15	0.21	1.37	0.52
pH	6.92	0.40	0.27	−0.60	0.06
Ca^{2+}	90.94	31.28	−0.27	−0.58	0.34
Mg^{2+}	18.88	11.68	0.61	−0.42	0.62
Na^{+}	58.05	29.54	−0.10	−0.76	0.51
K^{+}	12.58	5.46	−0.43	−0.72	0.43
Cl^{-}	13.87	15.24	2.56	7.29	1.10
SO_4	13.37	5.65	0.46	−0.68	0.42
N	13.69	11.00	1.25	0.59	0.80
F^{-}	121.95	48.14	0.46	−0.34	0.39
PO_4^{2-}	3.66	1.51	−1.16	2.60	0.41
$CaCO_3$	107.85	47.35	1.17	0.76	0.44
Fe	3.13	2.47	−0.34	−2.02	0.79
Cu^{2+}	0.18	0.11	0.18	−1.48	0.62
Cd	0.00	0.00	1.04	−1.22	1.61
Pb	0.00	0.00	0.57	−1.00	0.96
Zn	0.24	0.10	−0.25	−1.38	0.41
Cr	0.02	0.02	0.87	−0.17	1.02
Al	0.01	0.01	−0.33	−1.20	0.68
Ba	0.00	0.00	2.89	8.67	2.21
Mn^{2+}	0.08	0.08	0.56	−0.90	0.97

of the closeness of the wells to the open dumpsites (GW1 = 15 m, GW5 = 18.25 m, GW8 = 22.38 m & GW9 = 45 m). Surface run-off plays an important role in contaminating the water by depositing contaminants into the wells (Gurmessa et al., 2022; Huang et al., 1994).

Therefore, it can be concluded that the relatively weak acid to alkaline pH values recorded in the groundwater could be a result of the higher chloride, carbonate, and bicarbonate ions. The anion dominance was in the order of HCO_3^- + CO_3 > SO_4^{2-} > Cl^- + F, while the cations were in the order Ca^{2+} > Na^+ + K > Mg^{2+}. (Abugu et al., 2021; Ojekunle et al., 2020) observed the trend; Ca^{2+} > Na^+ + K > Mg^{2+} for the cations, while the anions were HCO_3^- > SO_4^{2-} > Cl^- > NO_3^- > CO_3^{2-} > PO_4^{3-}. These showed a slightly different order of major ions abundance within similar geological settings.

3.2. Water Quality for Domestic Use

The water quality index (WQI) was calculated by analyzing data collected from groundwater samples, applying a weighted approach arithmetic index method

for about eleven physicochemical parameters (EC, pH, TDS, Ca^{2+}, Mg^{2+}, Na^{+}, K^{+}, SO_4^{2-}, NO_3^{-}, Cl^{-}, PO_4^{3-}, and HCO_3^{-}). The WQI model adopted was precise in revealing the quality status of all the samples. The order of dominance for the ion concentration and the computed WQI with their classification are presented (**Table 5**). The results from the analysis of physicochemical factors showed that the groundwater sampled from GW1 and GW5 5 are not fit for consumption or other domestic uses due to the level of concentration above the permissible limit according to (WHO, 2022). However, the rest of the samples fell below the permissible limit, which demonstrated their suitability for consumption and other usage. The values obtained from the computed WQI showed that 70% of the samples were of good water quality, 10% were of excellent quality, and 20% were of poor quality (**Table 5**).

3.3. Hydrogeochemical Facies of the Groundwater of the Study Area

Hydrogeochemical facies are regions that have clearly defined boundaries and are distinguished by their unique combinations of cation and anion concentrations. These facies are categorized into distinct zones based on their specific chemical compositions (Appelo, & Postma 2005). The hydrogeochemical data can be interpreted using different graphical methods, such as Piper diagrams and Durov diagrams. Durov's plot enhances the understanding of hydrogeochemical facies by aiding in the identification of different water types and providing additional information about their characteristics (Durov, 1948). Additionally, it can demonstrate certain potential geochemical processes that aid in understanding and evaluating groundwater quality (Mukherjee et al., 2020). The Durov plot of the study area indicated that the groundwater in the region belongs to the Ca^{2+}-Mg^{2+}-CO_3-HCO_3-facies field (**Figure 3(a)**). This indicates that alkaline earth elements have a higher concentration and prevalence compared to alkali

Table 5. Water quality indices.

Code	Oder of dominance for major ions		WQI	Class
	Cation	Anion		
GW1	$Ca^{2+} > Na^{+} + K > Mg^{2+}$	$HCO_3^{-} + CO_3 > SO_4^{2} > Cl^{-} + F$	110.6	Poor
GW2	$Ca^{2+} > Na^{+} + K > Mg^{2+}$	$HCO_3^{-} + CO_3 > Cl^{-} + F > SO_4^{2}$	41.2	Good
GW3	$Ca^{2+} > Na^{+} + K > Mg^{2+}$	$HCO_3^{-} + CO_3 > SO_4^{2} > Cl^{-} + F$	61.1	Good
GW4	$Ca^{2+} > Na^{+} + K > Mg^{2+}$	$HCO_3^{-} + CO_3 > SO_4^{2} > Cl^{-} + F$	77.2	Good
GW5	$Ca^{2+} > Na^{+} + K > Mg^{2+}$	$HCO_3^{-} + CO_3 > SO_4^{2} > Cl^{-} + F$	110.6	Poor
GW6	$Ca^{2+} > Na^{+} + K > Mg^{2+}$	$HCO_3^{-} + CO_3 > SO_4^{2} > Cl^{-} + F$	56.2	Good
GW7	$Ca^{2+} > Na^{+} + K > Mg^{2+}$	$HCO_3^{-} + CO_3 > SO_4^{2} > Cl^{-} + F$	62.3	Good
GW8	$Ca^{2+} > Na^{+} + K > Mg^{2+}$	$HCO_3^{-} + CO_3 > Cl^{-} + F > SO_4^{2}$	73.3	Good
GW9	$Ca^{2+} > Na^{+} + K > Mg^{2+}$	$HCO_3^{-} + CO_3 > SO_4^{2} > Cl^{-} + F$	50.3	Good
GW10	$Ca^{2+} > Na^{+} + K > Mg^{2+}$	$HCO_3^{-} + CO_3 > SO_4^{2} > Cl^{-} + F$	38.5	Excellent

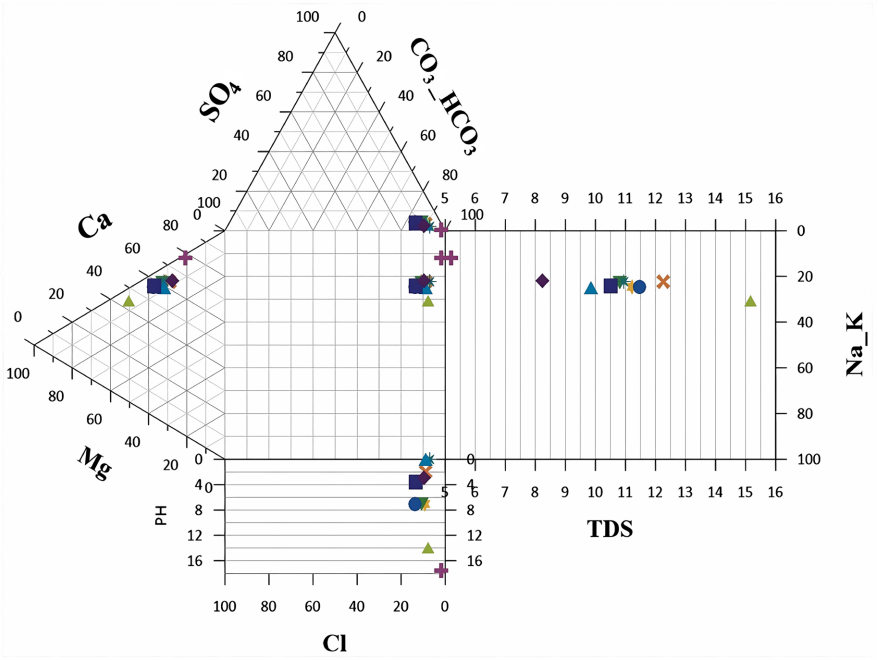

(a)

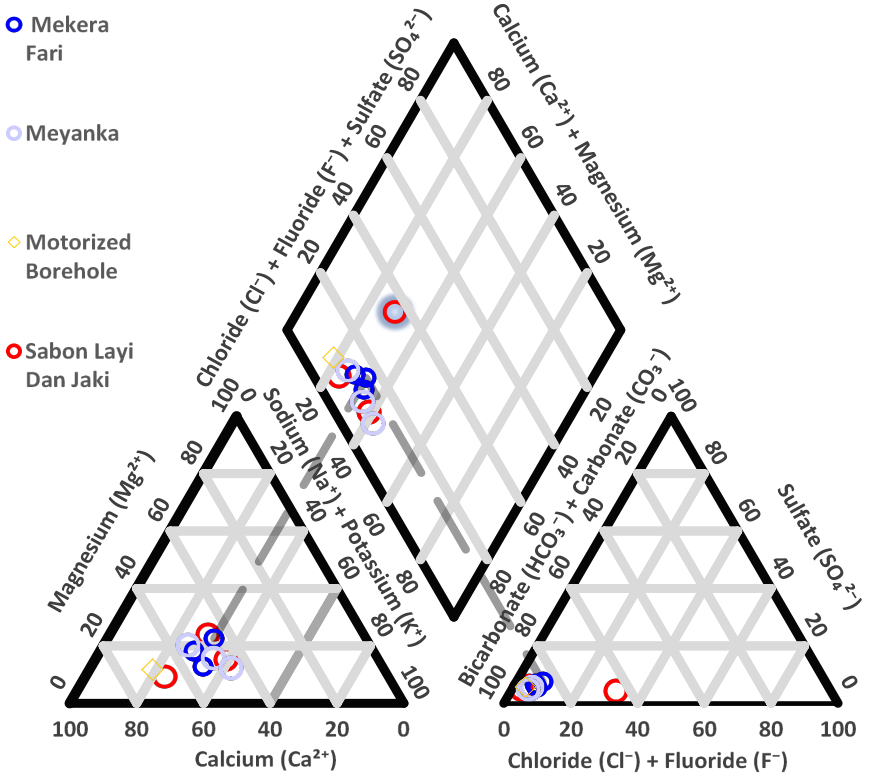

(b)

Figure 3. (a) Durov plot of groundwater values and (b) Piper plot of groundwater parameters.

elements in the region, while some of the samples shown were affected by the reverse ion exchange process.

The hydrogeochemical facies observed in natural water sources may be as a result of anthropogenic activities and geologic processes of the study area. The Piper diagram and the stiff plots of the dominant ions (measured in percentage milliequivalent per liter) of the water samples are presented **Figure 3(b)** and **Figure 4** respectively. The total ionic concentrations and water compositions of groundwater taken from various sources are described and compared using stiff plots based on the width and shape pattern on the stiff chart (**Figure 4**). On the other hand, the Piper diagram (**Figure 3(b)**) for the study area shows Ca^{2+}-Mg-HCO_3 Mg-HCO_3 as dominant water types from the samples analyzed. This indicates that water mineralization is a result of the probable dissolution of halite (Appelo, & Postma 2005). Other potential factors that may contribute to these phenomena include weathering, leaching, and cation exchange processes (Farid et al., 2015; Gurmessa et al., 2022). The dominance of Ca^{2+} over Na^{+} resulting from ion exchange could be linked to the weathering of ferromagnesian minerals in intrusive rocks (Akanbi, 2016), similar to those found in the area. These minerals, particularly the feldspars, are rich in calcium, sodium, and potassium.

The Gibbs diagram (**Figure 5(a)**) showed that the dominant factor responsible for the ions present in the water from the study area is weathering (Edet & Okereke, 2022; Xu et al., 2019) due to rock-water interaction. The majority of the analyzed samples were situated within the rock dominance region, indicating

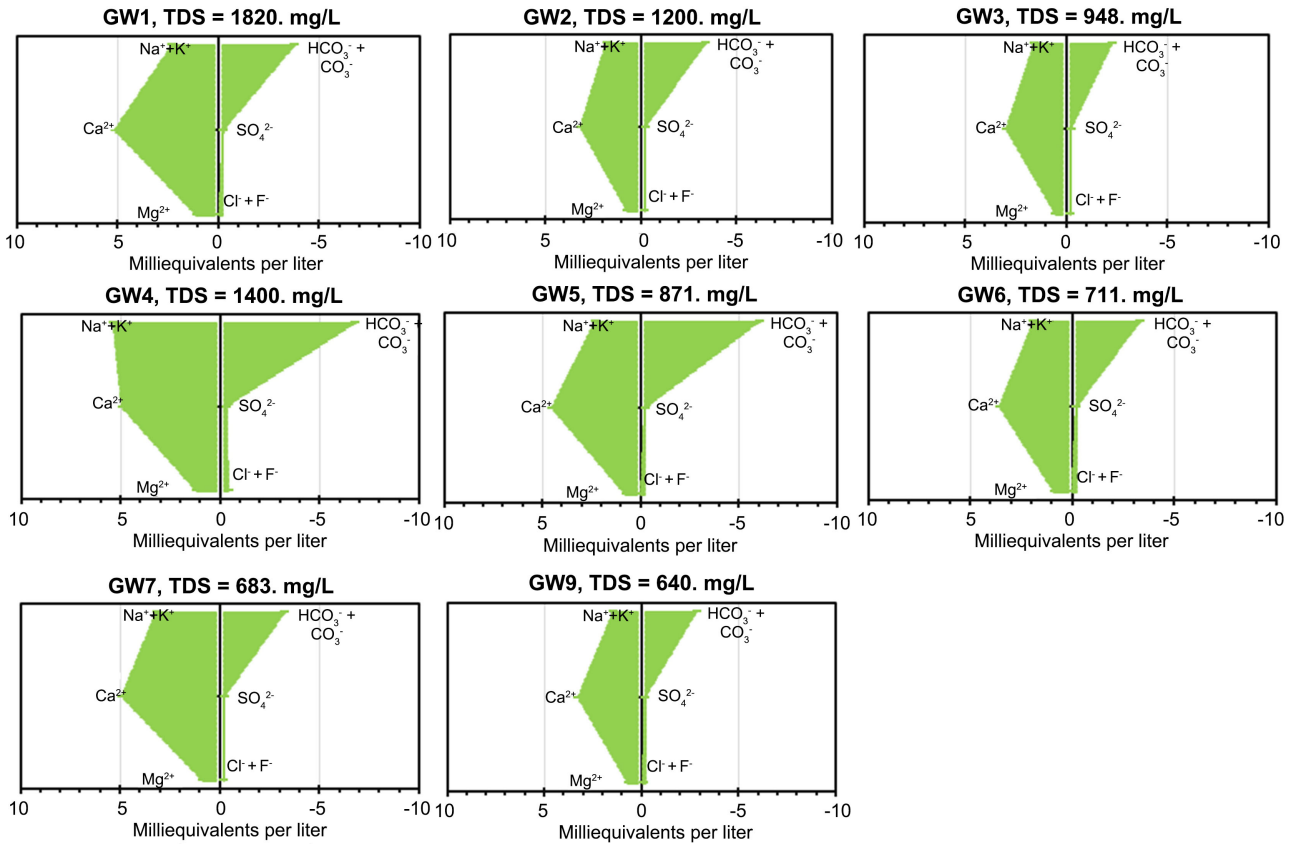

Figure 4. Stiff plots of groundwater ionic distribution.

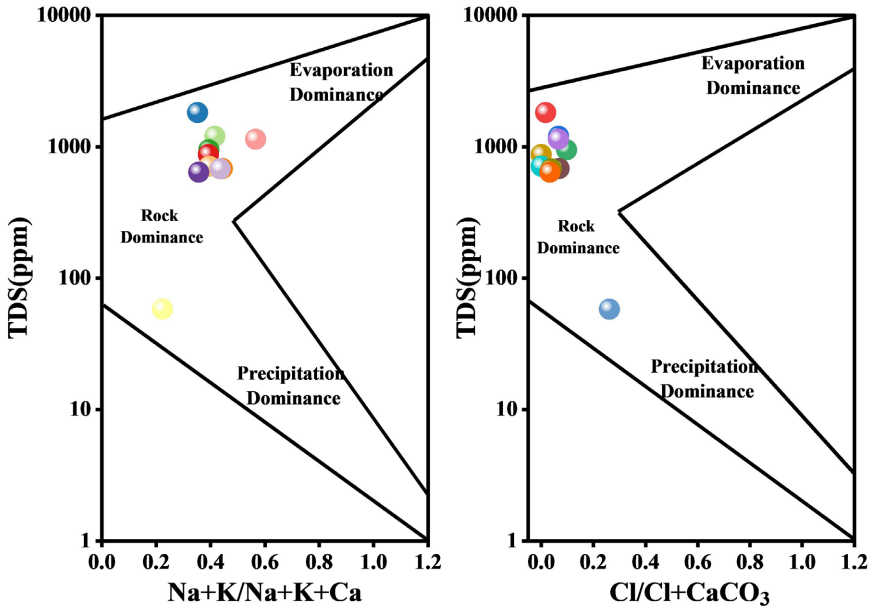

(a)

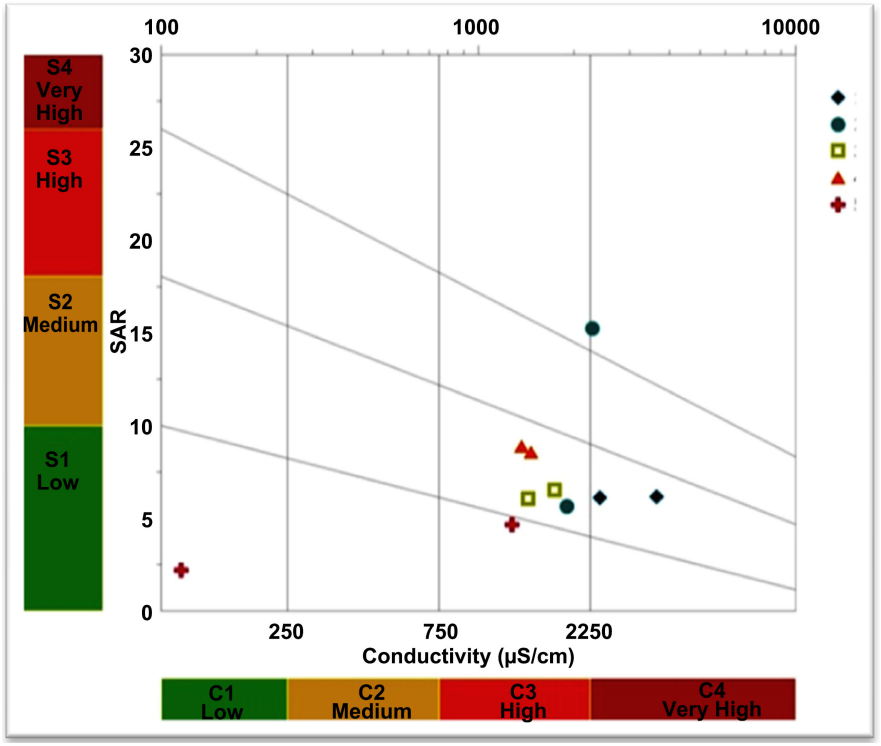

(b)

Figure 5. (a) Gibbs plot of groundwater controlling mechanisms and (b) Wilcox diagram depicting the suitability of the groundwater in the study area for agriculture.

that the enrichment of ion constituents in the groundwater is primarily attributed to the process of rock weathering and dissolution processes in soils or aquiferous materials along the groundwater flow path. Some of the samples were plotted towards the evaporation field, while one sample was plotted towards the

precipitation or rainfall dominance field, respectively. Generally, HCO_3^- and CO_3^{2-} were from carbonate rocks and dolomite of atmospheric origin (Egbueri, 2021). It can be concluded that the chemistry of groundwater is greatly influenced by weathering and cation exchange processes.

3.4. Water Suitability for Irrigation

Physical and chemical factors have the potential to interfere with plant metabolism and reduce soil permeability (Kumar et al., 2017). Hence, indices such as %Na, SAR, PI, and MH were employed to assess the suitability of the groundwater for agricultural purposes within the area of study (**Table 6**). (Sawyer & McCarthy, 1967) have defined classes for TH based on their range of values. The results shows that majority of the water samples in this study are relatively soft which means that they do not contain much chloride and sulphate salts of the alkaline earth metals (Gopinath et al., 2019), making it more suitable for agricultural purposes. Another important parameter used in evaluating water for irrigation is the percentage of sodium. About 60% of the samples fell within the "Good" field, 30% fell within the permissible field, and 10% fell within the "Excellent" for irrigation purposes (**Table 6**). EC is an important parameter for classifying irrigation water quality (Nematollahi et al., 2015). Thus, the Wilcox diagram (**Figure 5(b)**) was employed to classify the water samples analyzed for agricultural purposes. The diagram revealed that nearly all the samples appeared under a "good to permissible" field except for one sample that is classified as "doubtful to unsuitable" for irrigation purposes. The values of EC show a medium presence of sodium salts in the water, which, when in excess, limit air and water movement in the soil in the wet season (Ogunlaja et al., 2019; Ravikumar et al., 2010; Saleh et al., 1999). This indicates that water from Keffi Metropolis and its environs is suitable for agricultural purposes. SAR is also important in the evaluation of irrigation water as it plays a crucial role in determining soil permeability. Elevated

Table 6. Computed values of Na%, SAR, PI and MH in the study area.

Code	Na%	SAR	PI	MH
GW1	39.2	11.1	41.4	23.2
GW2	40.5	7.2	43.4	12.6
GW3	35.0	5.4	39.9	17.0
GW4	42.5	10.3	44.2	16.4
GW5	32.6	6.5	33.5	18.4
GW6	49.2	10.7	52.5	14.1
GW7	46.8	11.1	47.6	17.0
GW8	37.1	7.8	38.1	23.7
GW9	30.8	3.9	28.8	7.9
GW10	19.7	2.1	33.7	9.4

Na% = Percentage sodium value; SAR = Sodium Adsorption Ration; PI = Pollution index.

levels of sodium can lead to a reduction in the permeability of soil structure. Table 6 showed that SAR is less than 18 for all the groundwater sampled; 60% of the samples fell into the excellent category, while the remaining 40% fell under the Good category, respectively, indicating that the water of the study area is suitable for irrigation based on this index. Salinity is an expression of EC, and, in turn, a measure of the leaching of dissolved salts in water (Nematollahi et al., 2015).

The PI (Permeability Index) was also utilized to assess the suitability of water sources for irrigation. According to the analysis, all the examined samples were categorized as having a moderate suitability for irrigation purposes. Additionally, the MH (Magnesium to Calcium and Magnesium in water) ratio was employed to evaluate the potential impact on soil quality, as it can have implications for overall agricultural productivity. According to (Ravikumar et al., 2010), MH > 50% would negatively impact crop output as the soil becomes alkaline. In this study, the MH values obtained showed that all the water sampled was suitable for irrigation.

The correlation coefficient (r) between two variables shows how one variable predicts the other. The correlation coefficients of the tested parameters are listed in Table 7 and Figure 6(d). The main contributing ions in groundwater samples

Table 7. Pearson matrix for the groundwater.

	Ec (µS/cm)	pH	Ca^{2+}	Mg^{2+}	Na^{+}	K^{+}	Cl^{-}	SO_4	N	F	PO_4	$CaCO_3$	Fe	Cu++	Cd	Pb	Zn
Ec (µS/cm)	1																
pH	−0.40615	1															
Ca^{2+}	0.59141	−0.68836	1														
Mg^{2+}	0.72252	−0.43146	0.87141	1													
Na^{+}	0.3773	−0.34924	0.76139	0.78005	1												
K^{+}	0.41568	−0.53748	0.89542	0.82103	0.84548	1											
Cl^{-}	−0.36387	0.2	−0.3968	−0.41541	0.12761	−0.3122	1										
SO_4	0.74674	−0.34755	0.78207	0.87572	0.85552	0.81459	−0.14658	1									
N	0.52505	−0.17761	0.71796	0.83008	0.94584	0.81557	−0.00852	0.94215	1								
F	0.08285	−0.44053	0.12317	−0.14012	0.18971	0.10789	0.48529	0.09412	0.04487	1							
PO_4	0.61317	−0.41028	0.86326	0.90786	0.86217	0.91344	−0.28332	0.94854	0.91327	−0.06588	1						
$CaCO_3$	0.42078	−0.05819	0.64317	0.69477	0.75951	0.72523	−0.1025	0.73917	0.81726	0.21101	0.6887	1					
Fe	0.75223	0.21676	0.28114	0.50423	0.33282	0.22092	−0.13063	0.6744	0.58228	−0.05429	0.49371	0.58104	1				
Cu++	0.56058	−0.59935	0.85499	0.85206	0.70811	0.68241	−0.20495	0.69292	0.64082	−0.07763	0.77672	0.43957	0.25526	1			
Cd	−0.0199	0.11658	−0.01664	0.13533	−0.02969	0.10906	−0.16647	0.07528	0.03371	−0.5923	0.22934	−0.14356	0.02517	0.21759	1		
Pb	0.32926	−0.4284	0.73039	0.55159	0.61203	0.7558	−0.1437	0.59063	0.57049	0.45119	0.61235	0.80737	0.29183	0.49089	−0.08022	1	
Zn	−0.35736	0.20635	0.11272	0.05896	0.38052	0.10393	0.43376	0.01341	0.25133	−0.12164	0.09885	0.24002	−0.09795	0.29118	0.177	0.10508	1
Cr	0.72575	−0.5337	0.31496	0.24968	−0.08371	0.11419	−0.28364	0.32121	−0.00418	0.22382	0.2423	−0.05972	0.38978	0.31494	0.19113	0.22766	−0.5053
Al	0.6113	−0.54938	0.64582	0.60478	0.39581	0.51972	−0.30114	0.59141	0.41804	−0.17783	0.66854	0.11305	0.296	0.7232	0.52255	0.22784	0.08662
Ba	0.71767	−0.41398	0.35407	0.34119	−0.04404	−0.05293	−0.28024	0.24386	0.01132	0.04868	0.15231	−0.0484	0.41904	0.48667	−0.16333	0.05003	−0.25901
Mn^{2+}	0.27549	−0.60551	0.85885	0.60867	0.69347	0.79917	−0.1211	0.60293	0.58356	0.26675	0.71879	0.58324	0.11789	0.75441	0.0904	0.84889	0.31482

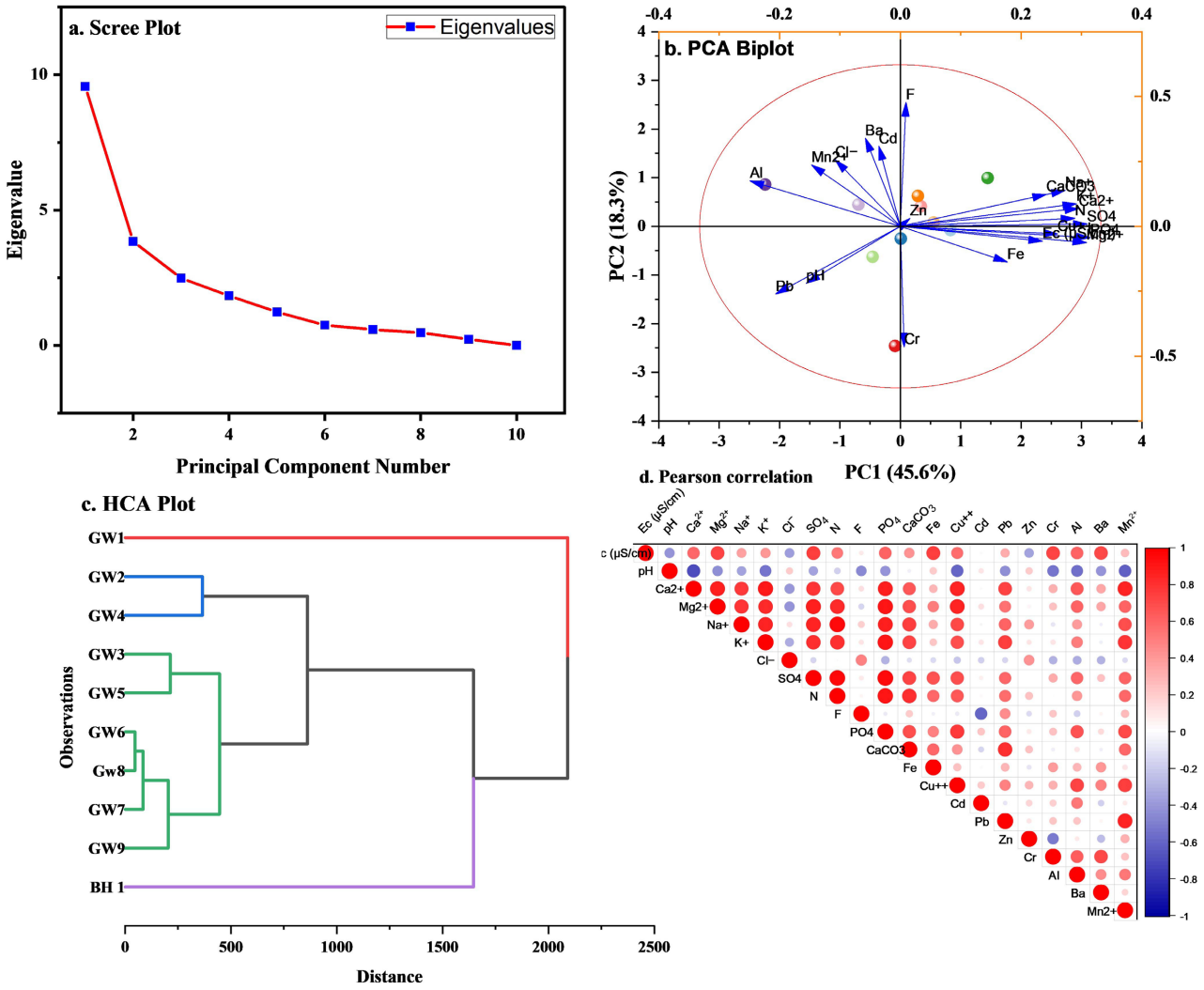

Figure 6. PCA scree plot (a), PCA biplot (b) and Hierarchical cluster plot (c), (d) Pearson correlation matrix.

that have a strong positive correlation with EC were Mg^{2+} (+0.72), SO_4^{2-} (+0.75), Fe (+0.75), Cr (0.73), and Ba^{2+} (0.71); those with a positive correlation with EC were Ca^{2+} (+0.59), N (+0.53), K^+ (+0.41), Cu^{2+} (+0.56), Al (+0.61), $CaCO_3$(+0.42); while it has a moderate positive correlation with EC are Na^+ (+0.38), F (+0.08), Pb (+0.33), Mn^{2+} (+0.28) respectively, However, pH exhibits a negative correlation with most of the heavy metals except for Fe (+0.22), Zn (0.21) and Cd (+0.11) exhibiting a positive correlation. This suggests that the groundwater of the study area is alkaline in nature and might be influenced by the chemical dissolution of the aquifer host rock or anthropogenic activities, as suggested by (Tahmasebi et al., 2018); (Abugu et al., 2021); (Edet & Okereke, 2022).

It was observed that Na^+ had a strong positive correlation with $CaCO_3$ (+0.76), PO_4^{3-} (+0.86) and K^+ (+0.85) and a moderate correlation with Cl^- (+0.23). The correlation expressed between Na^+ and Cl^- in the groundwater is an indication of salinization processes from geogenic and anthropogenic processes (Udiba. et al., 2016). K^+ concentration is very strongly correlated with $CaCO_3$ (+0.73),

SO_4^{2-} (+0.81), and PO_4^{3-} (+0.91); moderately negatively correlated with Cl^- (−0.31). Cl^- showed a negative low correlation with $CaCO_3$ (−0.10) and PO_4^{3-} (−0.28). This is a potential sign that anthropogenic inputs have contributed temporary and permanent hardness to the groundwater of the study area (Wali et al., 2019). Furthermore, a significant to moderate correlation between phosphate (PO_4^{3-}) and all the major ions examined further indicates the presence of anthropogenic contamination (Eldaw et al., 2021). This may arise from indiscriminate open waste dumps within the study area which is a common practice in most rural areas indicating anthropogenic influences (Edet & Okereke, 2022). Calcium carbonate ($CaCO_3$) positively correlated with sulphate (SO_4^{2-}) (+0.74) and phosphate (PO_4^{3-}) (+0.69), indicating the involvement of mineral dissolution processes of the host rock of the aquifer.

3.5. Source Discrimination

From the screen plot it can be determine that the first Principal Components (PC) covers most of the variance of the groundwater sampled analyses of the study area. This is followed by PC2 point which has moderately covered some variance while PC 3 capture the list as presented in **Figure 6(a)** respectively.

PCA was used to identify the different contamination sources influencing the heavy metal concentrations in the groundwater sampled in the study area. The first component (PC1) is explained by $CaCO_3$, Na^+, K^+ Ca^{2+}, and SO_4^{2-} accounts for 45.6% of the total variance of the analysis **Figure 6(b)**. This indicated that these metals could have contaminated the groundwater by anthropogenic activities as a result of seepage of leachates from open waste dumpsites into the wells (Shams et al., 2022). PC2 comprises of Ba^{2+}, Cd^{2+}, Cl^-, Mn^{2+} and Al^{3+} account for 18.3% of the total variance of the analysis. This indicates these metals originate from the same sources and could have been released through geogenic processes such as weathering at the aquifer.

HCA plot of the groundwater samples of the study area is presented in **Figure 6(c)**. A horizontal reference line is drawn at a distance of 0 - 2500 while the vertical line showed the classification of groups 1 to 4. Six (6) samples (60%) of the groundwater samples of the study area was categorized in group 1 (GW 3, 5, 6, 7, 8 & 9), while two (2) samples (20%) fell in group 2 (GW 2 and 4), One sample each was in groups 3 (BH1) and 4 (GW1) respectively. Each group exhibited different groundwater qualities, the Group 1 groundwater samples showed significant pollution compared to the Group 2 samples with moderate pollution while groups 3 & 4 depict insignificant pollution of the samples.

From the scatter plots (**Figure 7**), it is clearly shown that most of the tested parameters were strongly correlated with HCO_3^-. Moderate to positive correlation were found between Ca^{2+} and HCO_3 (r = 0.64), Mg^{2+} and HCO_3^- (r = 0.48) and K and HCO_3 (r = 0.46) The positive correlation between Ca^{2+}, Mg^{2+}, K^+, and HCO_3^- implies that as the concentration of HCO_3^- increases, there is a tendency for the concentrations of Ca^{2+}, Mg^{2+}, and K^+ increase, and vice versa. This

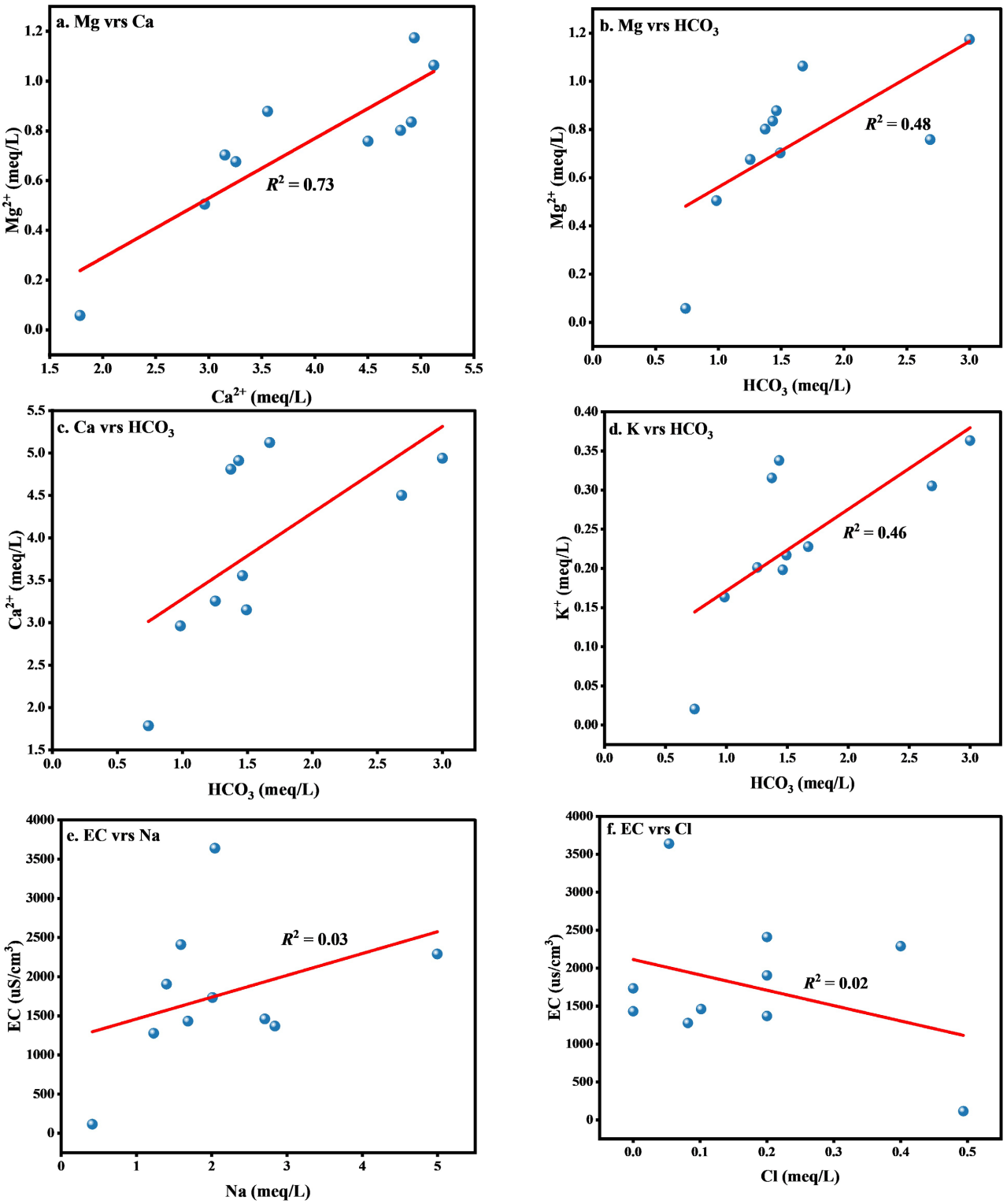

Figure 7. Scatter plots showing relationship between hydrochemical parameters.

indicates that there may be shared sources or processes influencing the mobility and availability of these ions in the hydrochemical system, which might be an indication that the aquifer may have experienced various processes such as wa-

ter–rock interaction, Carbonate Equilibrium and weathering of the aquifer's original rocks, therefore making HCO_3^- as a dominant ion in the water chemistry (Ogarekpe et al., 2023). There is positive correlation between Ca^{2+} and Mg^{2+} since the correlation coefficient (r) between two variables shows how one variable predicts the other. The correlation coefficients of the tested parameters are listed in **Figure 8**. It clearly depicts that most of the tested parameters were strongly correlated with HCO_3. Moderate to positive correlation existed between Ca and HCO_3 (r = 0.64), Mg and HCO_3 (r = 0.48) and K and HCO_3 (r = 0.46) The positive correlation between Ca, Mg, K, and HCO_3 implies that as the concentration of HCO_3 increases, there is a tendency for the concentrations of Ca,

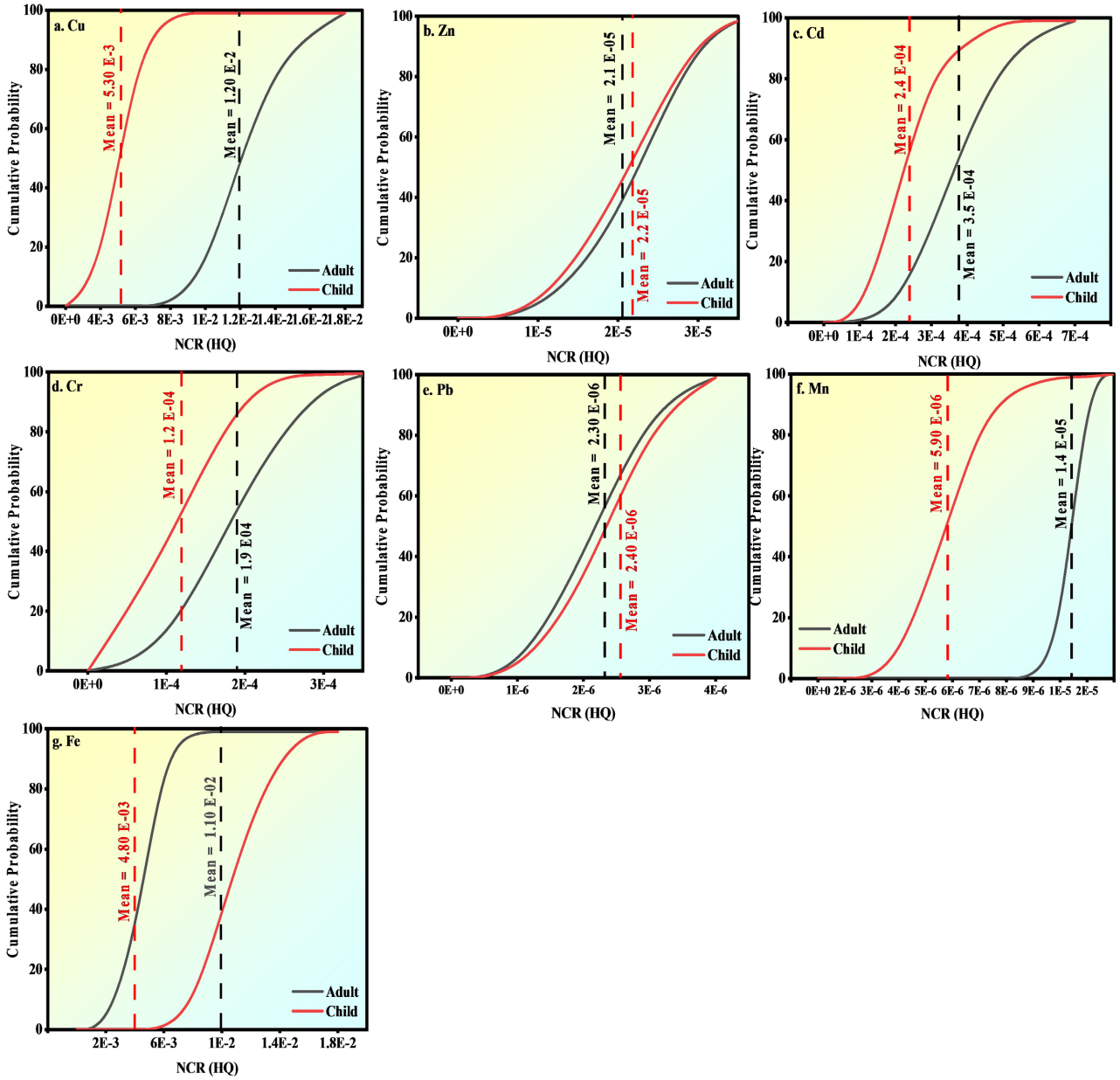

Figure 8. Cumulative probability distribution-NCR of heavy metals.

Mg, and K increase, and vice versa. This indicates that there may be shared sources or processes influencing the mobility and availability of these ions in the hydrochemical system, which might be an indication that the aquifer may have experienced various processes such as water-rock interaction, Carbonate Equilibrium and weathering of the aquifer's original rocks, therefore making HCO_3 as a dominant ion in the water chemistry (Ogarekpe et al., 2023). The positive correlation between Ca and Mg (r = 0.73) implies that as the concentration of Ca increases, there is a tendency for the concentration of Mg to increase, and vice versa. This suggests that there may be similar sources or processes influencing the mobility and availability of both Ca and Mg in the hydrochemical system such the local geology, water-rock interactions within the aquifer as well as anthropogenic Influences of the study area (Abdelshafy et al., 2019). The results show a low positive correlation between EC and Na^+ (r = 0.03), EC and Cl^- (r = 0.02). Based on these results, it suggests that there is little to no linear relationship between EC and the concentrations of Na^+ or Cl^-. The small positive correlation coefficients imply that as EC increases, there is a slight tendency for Na^+ and Cl^- concentrations to also increase, but the relationship is not strong or significant.

3.6. Health Risk Assessment

The health risks associated with heavy metals (Fe, Cu, Cd, Pb, Cr, Mn & Zn) present in groundwater, as well as their impacts on human health through various pathways were assessed. The study specifically examined the non-carcinogenic health risks for both adults and children in the study area, considering exposure through drinking water and dermal contact pathways. The calculated results of these health risks are presented and discussed in the study in **Table 8(a)** & **Table 8(b)** and **Table 9(a)** & **Table 9(b)** respectively. As shown in **Table 8(a)**, the non-carcinogenic health risk of heavy metals ranges from 2.44E−09 - 9.42E−08 for adults, and from 1.58E−10 - 8.52E−09 for children (ingestion), while for dermal, the value ranges from 1.40E−09 - 5.18E−11 for adults and from 1.16E−10 - 6.25E−09 for children, respectively. **Table 8(b)** shows that the hazard index (HI) of heavy metal had ranges of 1.35E−5 - 9.04E−08 for adults and 1.13E−07 - 8.55E−11 for children (ingestion), while for dermal, the value ranges were 7.01E−11 - 1.080E−07 for adults and 1.04E−05 - 8.04E−07 for children. The outcomes of the health risk assessment conducted in the study area, considering both adults and children, fall within the acceptable limit for non-carcinogenic risk.

Table 9(a) depicts the carcinogenic health risk of heavy metals for both adults and children in the study area. The value ranges from 1.51E−11 - 8.14E−10 for adults and 1.32E−11 - 7.10E−10 for children (ingestion), while for dermal, the value ranges from 8.63E−12 - 1.05E−09 for adults and 9.64E−12 - 1.18E−09 for children, respectively. **Table 9(b)** shows the total carcinogenic risk (TCR) of heavy metals for adults and children. All the values obtained were below the

Table 8. (a) Non-carcinogenic health risk of heavy metals to adults and children; (b) Hazard index (HI) of heavy metals to adults and children.

(a)

Heavy Metal	Ingestion		Dermal	
	Adult	Child	Adult	Child
Fe	9.42E−08	3.29E−07	5.39E−08	2.41E−07
Cu	5.51E−09	1.92E−08	3.16E−09	1.41E−08
Cd	9.04E−11	3.16E−10	5.18E−11	2.31E−10
Pb	4.52E−11	1.58E−10	2.59E−11	1.16E−10
Zn	7.34E−09	2.56E−08	4.21E−09	1.88E−08
Cr	7.05E−10	2.46E−09	4.04E−10	1.81E−09
Mn	2.44E−09	8.52E−09	1.40E−09	6.25E−09

(b)

Heavy Metal	Ingestion		Dermal	
	Adult	Child	Adult	Child
Fe	1.35E−05	4.70E−05	1.80E−07	8.04E−07
Cu	1.38E−10	4.81E−10	2.63E−10	1.18E−09
Cd	9.04E−08	3.16E−07	5.18E−06	2.31E−05
Pb	3.23E−08	1.13E−07	6.16E−11	2.76E−10
Zn	2.45E−11	8.55E−11	7.01E−11	3.13E−10
Cr	2.35E−07	8.21E−07	2.69E−07	1.20E−06
Mn	1.74E−08	6.09E−08	2.33E−06	1.04E−05

Table 9. (a) Carcinogenic health risk of heavy metals to adults and children; (b) Total carcinogenic risk (TCR) of heavy metals to adults and children.

(a)

Heavy Metal	Ingestion		Dermal	
	Adult	Child	Adult	Child
Fe	3.14E−08	2.74E−08	1.80E−08	2.01E−08
Cu	1.84E−09	1.60E−09	1.05E−09	1.18E−09
Cd	3.01E−11	2.63E−11	1.73E−11	1.93E−11
Pb	1.51E−11	1.32E−11	8.63E−12	9.64E−12
Zn	2.45E−09	2.14E−09	1.40E−09	1.57E−09
Cr	2.35E−10	2.05E−10	1.35E−10	1.50E−10
Mn	8.14E−10	7.10E−10	4.66E−10	5.21E−10

(b)

Heavy Metal	Ingestion	
	Adult	Child
Fe	6.28E−07	5.48E−07
Cd	1.84E−10	1.60E−10
Pb	1.28E−13	1.12E−13
Cr	2.00E−12	1.74E−12

standard permissible limit for human health risks from heavy metals (De et al., 2023). However, it should be concluded that continuing to use the water in the study area may not affect the health of the community. Additionally, the results of the cumulative probability distribution of non-carcinogenic heavy metals in the study area are shown in (**Figure 8**). It can be seen from Figure that the total non-carcinogenic risks for adults and children were virtually below the permissible limits. In general, the non-carcinogenic health risk of heavy metals in the groundwater was found to be low in the study area. However, serious precautions should be taken to curtail the risk of people becoming prone to disease in the future.

4. Conclusion

The study showed that the average values of all the parameters assessed in the study area were within the WHO standard for drinking water. The sequence for the anion dominance was $HCO_3^- + CO_3 > SO_4^{2-} > Cl^- + F$, while the order for cations was $Ca^{2+} > Na^+ + K > Mg^{2+}$ in the groundwater. The WQI computed indicates that the groundwater of the study area is suitable for domestic purposes, as it was classified as generally having good to excellent water quality. The hydro-chemical facies for this study area is, namely; Ca-Mg-HCO_3 dominant water type from the samples analyzed. Indices such as %Na, PI, SAR, and MH, indicate that water sources from Keffi Metropolis and environs are adequate for irrigation.

Health risk assessment revealed that both children and adults would not be affected much by the ingestion of the current heavy metal in the groundwater samples. However, the results of this investigation are limited to the heavy metals leachate from waste dumpsites, further research on Pesticides and organic pollutant as well as other contaminants of groundwater in the vicinity of dumpsites has been considered and future research in the study area will consider the interaction of heavy metals and pesticides to human health risk in the Keffi metropolis. Therefore, it is recommended that periodic assessments of these ions and other pollutants be carried out. There is a need for the authorities (State and Local Government) to provide clean, adequate pipe borne water for the community, and appropriate, timely measures should be taken towards proper management of open waste dumpsites to prevent the contamination of groundwater.

Funding

This research was supported by the Natural Science Foundation of China (No. 21377098) and Most Key Program of China (2018YFC1803100).

Credit Authorship and Contribution Statement

Kyari Umar Donuma: Investigation, Data curation, Writing-original draft preparation. Limin Ma: Supervision, Validation, Funding, Project administration, Supervision, Resources, Validation, Funding, Writing-review & editing. Chengcheng Bu

and Lartey-Young George: Writing-review and editing.

Ethical Approval

All authors have read, understood, and have complied as applicable with the statement on "Ethical responsibilities of Authors" as found in the Instructions for Authors and are aware that with minor exceptions, no changes can be made to authorship once the paper is submitted.

Data Availability

The authors do not have permission to share data.

Acknowledgements

This research was supported by the Natural Science Foundation of China (No. 21377098) and Most Key Program of China (2018YFC1803100).

Conflicts of Interest

The authors declare they have no competing financial interests or personal relationships that could have appeared to influence the work reported in this paper.

References

Abdelshafy, M., Saber, M., Abdelhaleem, A., Abdelrazek, S. M., & Seleem, E. M. (2019). Hydrogeochemical Processes and Evaluation of Groundwater Aquifer at Sohag City, Egypt. *Scientific African, 6,* e00196. https://doi.org/10.1016/j.sciaf.2019.e00196

Aboyeji, O. S., & Eigbokhan, S. F. (2016). Evaluations of Groundwater Contamination by Leachates around Olusosun Open Dumpsite in Lagos Metropolis, Southwest Nigeria. *Journal of Environmental Management, 183,* 333-341. https://doi.org/10.1016/j.jenvman.2016.09.002

Abugu, H. O., Egwuonwu, P. F., Ihedioha, J. N., & Ekere, N. R. (2021). Hydrochemical Evaluation of River Ajali Water for Irrigational Application in Agricultural Farmland. *Applied Water Science, 11,* Article No. 71. https://doi.org/10.1007/s13201-021-01395-4

Akanbi (2016). Use of Vertical Electrical Geophysical Method for Spatial Characterisation of Groundwater Potential of Crystalline Crust of Igboora Area, Southwestern Nigeria. *International Journal of Science and Research, 6,* 399-406. https://www.ijsrp.org/research-paper-0316/ijsrp-p5164.pdf

Akinbile, C. O., & Yusoff, M. S. (2011). Environmental Impact of Leachate Pollution on Groundwater Supplies in Akure, Nigeria. *International Journal of Environmental Science and Development, 2,* 81-86. https://doi.org/10.7763/IJESD.2011.V2.101

Akter, T., Jhohura, F. T., Akter, F., Chowdhury, T. R., Mistry, S. K., Dey, D., & Rahman, M. (2016). Water Quality Index for Measuring Drinking Water Quality in Rural Bangladesh: A Cross-Sectional Study. *Journal of Health, Population and Nutrition, 35,* Article No. 4. https://doi.org/10.1186/s41043-016-0041-5

Appelo, C. A. J., & Postma, D. (2005). *Geochemistry, Groundwater and Pollution*. CRC Press. https://doi.org/10.1201/9781439833544

Aromolaran, O., Fagade, O. E., Aromolaran, O. K., Faleye, E. T., & Faerber, H. (2019). Assessment of Groundwater Pollution near Aba-Eku Municipal Solid Waste Dumpsite.

Environmental Monitoring and Assessment, 191, Article No. 718. https://doi.org/10.1007/s10661-019-7886-1

Bolujoko, N. B., Ogunlaja, O. O., Alfred, M. O., Okewole, D. M., Ogunlaja, A., Olukanni, O. D., & Unuabonah, E. I. (2022). Occurrence and Human Exposure Assessment of Parabens in Water Sources in Osun State, Nigeria. *Science of the Total Environment, 814,* Article ID: 152448. https://doi.org/10.1016/j.scitotenv.2021.152448

Custodio, M., Cuadrado, W., Peñaloza, R., Montalvo, R., Ochoa, S., & Quispe, J. (2020). Human Risk from Exposure to Heavy Metals and Arsenic in Water from Rivers with Mining Influence in the Central Andes of Peru. *Water, 12,* Article No. 1946. https://doi.org/10.3390/w12071946

De, A., Das, A., Joardar, M., Mridha, D., Majumdar, A., Das, J., & Roychowdhury, T. (2023). Investigating Spatial Distribution of Fluoride in Groundwater with Respect to Hydro-Geochemical Characteristics and Associated Probabilistic Health Risk in Baruipur Block of West Bengal, India. *Science of the Total Environment, 886,* Article ID: 163877. https://doi.org/10.1016/j.scitotenv.2023.163877

Durov, S. A. (1948). *Classification of Natural Waters and Graphical Representation of Their Composition* (2nd ed.). Doklady Akademii Nauk SSSR.

Duru, R. U., Ikpeama, E. E., & Ibekwe, J. A. (2019). Challenges and Prospects of Plastic Waste Management in Nigeria. *Waste Disposal & Sustainable Energy, 1,* 117-126. https://doi.org/10.1007/s42768-019-00010-2

Edet, A., & Okereke, C. (2022). Investigation of Hydrogeological Conditions of a Fractured Shale Aquifer in Yala Area (Se Nigeria) Characterized by Saline Groundwater. *Applied Water Science, 12,* Article No. 194. https://doi.org/10.1007/s13201-022-01715-2

Egbueri, J. C. (2021). Signatures of Contamination, Corrosivity and Scaling in Natural Waters from a Fast-Developing Suburb (Nigeria): Insights into Their Suitability for Industrial Purposes. *Environment, Development and Sustainability, 23,* 591-609. https://doi.org/10.1007/s10668-020-00597-1

Eldaw, E., Huang, T., Mohamed, A. K., & Mahama, Y. (2021). Classification of Groundwater Suitability for Irrigation Purposes Using a Comprehensive Approach Based on the ahp and gis Techniques in North Kurdufan Province, Sudan. *Applied Water Science, 11,* Article No. 126. https://doi.org/10.1007/s13201-021-01443-z

Farid, I., Zouari, K., Rigane, A., & Beji, R. (2015). Origin of the Groundwater Salinity and Geochemical Processes in Detrital and Carbonate Aquifers: Case of Chougafiya Basin (Central Tunisia). *Journal of Hydrology, 530,* 508-532. https://doi.org/10.1016/j.jhydrol.2015.10.009

Ghaderpoori, M., Kamarehie, B., Jafari, A., Alinejad, A. A., Hashempour, Y., Saghi, M. H., & Ferrante, M. (2020). Health Risk Assessment of Heavy Metals in Cosmetic Products Sold in Iran: The Monte Carlo Simulation. *Environmental Science and Pollution Research, 27,* 7588-7595. https://doi.org/10.1007/s11356-019-07423-w

Gopinath, S., Srinivasamoorthy, K., Saravanan, K., & Prakash, R. (2019). Tracing Groundwater Salinization Using Geochemical and Isotopic Signature in Southeastern Coastal Tamilnadu, India. *Chemosphere, 236,* Article ID: 124305. https://doi.org/10.1016/j.chemosphere.2019.07.036

Gurmessa, S. K., MacAllister, D. J., White, D., Ouedraogo, I., Lapworth, D., & MacDonald, A. (2022). Assessing Groundwater Salinity across Africa. *Science of the Total Environment, 828,* Article ID: 154283. https://doi.org/10.1016/j.scitotenv.2022.154283

Huang, W.-Y., Beach, E. D., Fernandez-Cornejo, J., & Uri, N. D. (1994). An Assessment of the Potential Risks of Groundwater and Surface Water Contamination by Agricul-

tural Chemicals Used in Vegetable Production. *Science of the Total Environment, 153,* 151-167. https://doi.org/10.1016/0048-9697(94)90112-0

Ifeoluwa, O. B. (2019). Harmful Effects and Management of Indiscriminate Solid Waste Disposal on Human and Its Environment in Nigeria: A Review. *Global Journal of Research and Review.*

Kayode, O. T., Okagbue, H. I., & Achuka, J. A. (2018). Water Quality Assessment for Groundwater around a Municipal Waste Dumpsite. *Data in Brief, 17,* 579-587. https://doi.org/10.1016/j.dib.2018.01.072

Kshetrimayum, K. S., & Laishram, P. (2020). Assessment of Surface Water and Groundwater Interaction Using Hydrogeology, Hydrochemical and Isotopic Constituents in the Imphal River Basin, Northeast India. *Groundwater for Sustainable Development, 11,* Article ID: 100391. https://doi.org/10.1016/j.gsd.2020.100391

Kumar, V., Bharti, P. K., Talwar, M., Tyagi, A. K., & Kumar, P. (2017). Studies on High Iron Content in Water Resources of Moradabad District (up), India. *Water Science, 31,* 44-51. https://doi.org/10.1016/j.wsj.2017.02.003

Mangimbulude, J. C., Breukelen, B. M. V., Krave, A. S., Straalen, N. M. V., & Röling, W. F. M. (2009). Seasonal Dynamics in Leachate Hydrochemistry and Natural Attenuation in Surface Run-Off Water from a Tropical Landfill. *Waste Management, 29,* 829-838. https://doi.org/10.1016/j.wasman.2008.06.020

Masindi, V., & Foteinis, S. (2021). Groundwater Contamination in Sub-Saharan Africa: Implications for Groundwater Protection in Developing Countries. *Cleaner Engineering and Technology, 2,* Article ID: 100038. https://doi.org/10.1016/j.clet.2020.100038

McGeorge, W. T. (1954). Diagnosis and Improvement of Saline and Alkaline Soils. *Soil Science Society of America Journal, 18,* 348-348. https://doi.org/10.2136/sssaj1954.03615995001800030031x

Meng, T., Cheng, W., Wan, T., Wang, M., Ren, J., Li, Y., & Huang, C. (2021). Occurrence of Antibiotics in Rural Drinking Water and Related Human Health Risk Assessment. *Environmental Technology, 42,* 671-681. https://doi.org/10.1080/09593330.2019.1642390

Mishra, S., Tiwary, D., & Ohri, A. (2018). Leachate Characterisation and Evaluation of Leachate Pollution Potential of Urban Municipal Landfill Sites. *IJEWM, 4,* 217. https://doi.org/10.1504/IJEWM.2018.093431

Mukherjee, I., Singh, U. K., Singh, R. P., Anshumali, Kumari, D., Jha, P. K., & Mehta, P. (2020). Characterization of Heavy Metal Pollution in an Anthropogenically and Geologically Influenced Semi-Arid Region of East India and Assessment of Ecological and Human Health Risks. *Science of the Total Environment, 705,* Article ID: 135801. https://doi.org/10.1016/j.scitotenv.2019.135801

Munagala, S., Jagarapu, D. C. K. et al. (2020). Determination of Water Quality Index for Ground Water near Municipal Dump Site in Guntur. *Materials Today: Proceedings, 33,* 724-727. https://doi.org/10.1016/j.matpr.2020.06.030

Nematollahi, M. J., Ebrahimi, P., Razmara, M., & Ghasemi, A. (2015). Hydrogeochemical Investigations and Groundwater Quality Assessment of Torbat-Zaveh Plain, Khorasan Razavi, Iran. *Environmental Monitoring and Assessment*, *188*, Article No. 2 https://doi.org/10.1007/s10661-015-4968-6

Nyirenda, J., & Mwansa, P. M. (2022). Impact of Leachate on Quality of Ground Water around Chunga Landfill, Lusaka, Zambia and Possible Health Risks. *Heliyon, 8,* e12321. https://doi.org/10.1016/j.heliyon.2022.e12321

Ogarekpe, N. M., Nnaji, C. C., Oyebode, O. J., Ekpenyong, M. G., Ofem, O. I., Tenebe, I.

T., & Asitok, A. D. (2023). Groundwater Quality Index and Potential Human Health Risk Assessment of Heavy Metals in Water: A Case Study of Calabar Metropolis, Nigeria. *Environmental Nanotechnology, Monitoring & Management, 19,* Article ID: 100780. https://doi.org/10.1016/j.enmm.2023.100780

Ogunlaja, A., Ogunlaja, O. O., Okewole, D. M., & Morenikeji, O. A. (2019). Risk Assessment and Source Identification of Heavy Metal Contamination by Multivariate and Hazard Index Analyses of a Pipeline Vandalised Area in Lagos State, Nigeria. *Science of the Total Environment, 651,* 2943-2952. https://doi.org/10.1016/j.scitotenv.2018.09.386

Ojekunle, Z. O., Adeyemi, A. A., Taiwo, A. M., Ganiyu, S. A., & Balogun, M. A. (2020). Assessment of Physicochemical Characteristics of Groundwater within Selected Industrial Areas in Ogun State, Nigeria. *Environmental Pollutants and Bioavailability, 32,* 100-113. https://doi.org/10.1080/26395940.2020.1780157

Olufemi, O. S., Joshua, M. I., & Abraham Salamatu, E. (2021). Assessment of Temperature Variability Effect on Rice Production in Nasarawa State, Nigeria. *International Journal of Environment and Climate Change, 10,* 91-100. https://doi.org/10.9734/ijecc/2020/v10i830221

Omeka, M. E., & Egbueri, J. C. (2023). Hydrogeochemical Assessment and Health-Related Risks Due to Toxic Element Ingestion and Dermal Contact within the Nnewi-Awka Urban Areas, Nigeria. *Environmental Geochemistry and Health, 45,* 2183-2211. https://doi.org/10.1007/s10653-022-01332-7

Pejman, A., Nabi Bidhendi, G., Ardestani, M., Saeedi, M., & Baghvand, A. (2017). Fractionation of Heavy Metals in Sediments and Assessment of Their Availability Risk: A Case Study in the Northwestern of Persian Gulf. *Marine Pollution Bulletin, 114,* 881-887. https://doi.org/10.1016/j.marpolbul.2016.11.021

Pona, H. T., Xiaoli, D., Ayantobo, O. O., & Narh Daniel, T. (2021). Environmental Health Situation in Nigeria: Current Status and Future Needs. *Heliyon, 7,* e06330. https://doi.org/10.1016/j.heliyon.2021.e06330

Qiu, H., Gui, H., Xu, H., Cui, L., & Yu, H. (2023). Occurrence, Controlling Factors and Noncarcinogenic Risk Assessment Based on Monte Carlo Simulation of Fluoride in Mid-Layer Groundwater of Huaibei Mining Area, North China. *Science of the Total Environment, 856,* Article ID: 159112. https://doi.org/10.1016/j.scitotenv.2022.159112

Ravikumar, P., Venkatesharaju, K., Prakash, K., & Somashekar, R. K. (2010). Geochemistry of Groundwater and Groundwater Prospects Evaluation, Anekal Taluk, Bangalore Urban District, Karnataka, India. *Environmental Monitoring and Assessment, 179,* 93-112. https://doi.org/10.1007/s10661-010-1721-z

Saleh, A., Al-Ruwaih, F., & Shehata, M. (1999). Hydrogeochemical Processes Operating within the Main Aquifers of Kuwait. *Journal of Arid Environment, 42,* 195-209. https://doi.org/10.1006/jare.1999.0511

Sanga, V. F., Fabian, C., & Kimbokota, F. (2023). Heavy Metal Pollution in Leachates and Its Impacts on the Quality of Groundwater Resources around Iringa Municipal Solid Waste Dumpsite. *Environmental Science and Pollution Research, 30,* 8110-8122. https://doi.org/10.1007/s11356-022-22760-z

Sawyer, G. N., & McCarthy, D. L. (1967). *Chemistry of Sanitary Engineers*. McGraw Hill.

Shams, M., Tavakkoli Nezhad, N., Dehghan, A., Alidadi, H., Paydar, M., Mohammadi, A. A., & Zarei, A. (2022). Heavy Metals Exposure, Carcinogenic and Non-Carcinogenic Human Health Risks Assessment of Groundwater around Mines in Joghatai, Iran. *International Journal of Environmental Analytical Chemistry, 102,* 1884-1899. https://doi.org/10.1080/03067319.2020.1743835

Sheng, D., Meng, X., Wen, X., Wu, J., Yu, H., & Wu, M. (2022). Contamination Characteristics, Source Identification, and Source-Specific Health Risks of Heavy Metal (loid)s in Groundwater of an Arid Oasis Region in Northwest China. *Science of the Total Environment, 841,* Article ID: 156733. https://doi.org/10.1016/j.scitotenv.2022.156733

Siddiqua, A., Hahladakis, J. N., & Al-Attiya, W. A. K. A. (2022). An Overview of the Environmental Pollution and Health Effects Associated with Waste Landfilling and Open Dumping. *Environmental Science and Pollution Research, 29,* 58514-58536. https://doi.org/10.1007/s11356-022-21578-z

Singh, S., Raju, N. J., Gossel, W., & Wycisk, P. (2016). Assessment of Pollution Potential of Leachate from the Municipal Solid Waste Disposal Site and Its Impact on Groundwater Quality, Varanasi Environs, India. *Arabian Journal of Geosciences, 9,* Article No. 131. https://doi.org/10.1007/s12517-015-2131-x

Sufiyan, I., Mohammed, K., Bello, I., & Isa, Z. (2020). Impact of Harmattan Season on Human Health in Keffi, Nasarawa State, Nigeria. *Matrix Science Medica, 4,* 44-50. https://doi.org/10.4103/MTSM.MTSM_1_20

Tahmasebi, P., Mahmudy-Gharaie, M. H., Ghassemzadeh, F., & Karimi Karouyeh, A. (2018). Assessment of Groundwater Suitability for Irrigation in a Gold Mine Surrounding Area, NE Iran. *Environmental Earth Sciences, 77,* Article No. 766. https://doi.org/10.1007/s12665-018-7941-1

Thongyuan, S., Khantamoon, T., Aendo, P., Binot, A., & Tulayakul, P. (2021). Ecological and Health Risk Assessment, Carcinogenic and Non-Carcinogenic Effects of Heavy Metals Contamination in the Soil from Municipal Solid Waste Landfill in Central, Thailand. *Human and Ecological Risk Assessment: An International Journal, 27,* 876-897. https://doi.org/10.1080/10807039.2020.1786666

Tian, R., & Wu, J. (2019). Groundwater Quality Appraisal by Improved Set Pair Analysis with Game Theory Weightage and Health Risk Estimation of Contaminants for Xuecha Drinking Water Source in a Loess Area in Northwest China. *Human and Ecological Risk Assessment: An International Journal, 25,* 132-157. https://doi.org/10.1080/10807039.2019.1573035

Todd, K. D., & Mays, L. W. (2004). *Groundwater Hydrology* (3rd ed.). John Wiley and Sons.

Tyagi, S., Sharma, B., Singh, P., & Dobhal, R. (2013). Water Quality Assessment in Terms of Water Quality Index. *American Journal of Water Resources, 1,* 34-38. https://doi.org/10.12691/ajwr-1-3-3

U.S. EPA (2003). *Framework for Cumulative Risk Assessment*.

Udiba, U., Udofia, L. E., EzikeNkechi, N., Samuel, U., & Science, B. (2016). Assessment of the Impact of Solid Waste Dumps on Ground Water Quality, Calabar Municipality, Nigeria. *Journal of Advance Research in Pharmacy & Biological Science, 2*.

Wali, S. U., Umar, K. J., Abubakar, S. D., Ifabiyi, I. P., Dankani, I. M., Shera, I. M., & Yauri, S. G. (2019). Hydrochemical Characterization of Shallow and Deep Groundwater in Basement Complex Areas of Southern Kebbi State, Sokoto Basin, Nigeria. *Applied Water Science, 9,* Article No. 169. https://doi.org/10.1007/s13201-019-1042-5

WHO (2022). *Guidelines for Drinking-Water Quality. Fourth Edition Incorporating the First and Second Addenda*. https://www.who.int/publications/i/item/9789240045064

Xu, P., Feng, W., Qian, H., & Zhang, Q. (2019). Hydrogeochemical Characterization and Irrigation Quality Assessment of Shallow Groundwater in the Central-Western Guanzhong Basin, China. *International Journal of Environmental Research and Public Health, 16,* Article No. 1492. https://doi.org/10.3390/ijerph16091492

Yau, T., Asamoah, D., & Adam, M. (2013). Geochemistry and Petrogenesis of the Orthogneisses of Keffi Area, North Central, Nigeria. *Energy & Environmental Science, 127,* 387-393.